Journal of Applied Microbiology

Journal of Applied Microbiology ISSN 1364-5072

ORIGINAL ARTICLE

Honeybee glands as possible infection reservoirs of *Nosema ceranae* and *Nosema apis* in naturally infected forager bees

T.R. Copley and S.H. Jabaji

Plant Science Department, McGill University, Ste-Anne-de-Bellevue, QC, Canada

Keywords
honeybee glands, multiplex qPCR, Nosemosis, seasonal distribution patterns of *Nosema* species.

Correspondence
Suha H. Jabaji, Plant Science Department, McGill University, 21,111 Lakeshore, Ste-Anne-de-Bellevue, QC, Canada H9X 3V9.
E-mail: suha.jabaji@mcgill.ca

2011/1542: received 12 September 2011, revised 25 October 2011 and accepted 28 October 2011

doi:10.1111/j.1365-2672.2011.05192.x

Abstract

Aims: To determine whether *Nosema ceranae* and *Nosema apis* are present in different gland tissues of honeybee, *Apis mellifera* L. and to monitor spore presence and quantity in these glands in naturally infected hives from July 2009 to July 2010 in Quebec, Canada.

Methods and Results: *Nosema* spp. were quantified using duplex quantitative real-time PCR in the thoracic salivary, hypopharyngeal, mandibular glands, and venom sac and glands of *A. mellifera* over a period of 8 months. Both *Nosema* species were present in all the glands as single or mixed species; however, *N. apis* was not present as single-species detections in the salivary glands (see Table 2). *Nosema ceranae* was more prevalent throughout the 8 months. Significant correlative relationships were established for *N. ceranae* and *N. apis* levels in the honeybee glands and those found within the intestines of forager honeybees. Overall, the seasonality of *N. ceranae* and *N. apis* in the different glands tightly followed the seasonal patterns in the honeybee guts.

Conclusions: *Nosema ceranae* and *N. apis* are not tissue specific, and honeybee glands have potential to become a useful indicator of the extent of disease in the colony and may represent a potential infection reservoir.

Significance and Impact of the Study: First report of spore load quantification of *Nosema* spp. in different honeybee glands.

Introduction

Microsporidia are obligatory intracellular fungal parasites that are commonly found in insects and other invertebrates (Keeling and Fast 2002). For European honey bees (*Apis mellifera* L.), two species belonging to the genus *Nosema* have been confirmed as the causal agent of Nosemosis, a serious disease of honeybees and occurring in nearly every country where apiculture is practiced (Klee *et al.* 2007). This disease can cause significant economical damage to the apiculture industry if left untreated (Martín-Hernández *et al.* 2007; Higes *et al.* 2008). Both *Nosema* species infect primarily the midgut epithelium of adult honeybees causing swollen abdomens that limit nutrient absorption, increase energy demands and may cause dysentery (Mayack and Naug 2009, 2010; Fries 2010). The biology and epidemiology of *Nosema apis* is well established; however, the epidemiology and many biological features of *Nosema ceranae*, an emergent pathogen of *A. mellifera*, remain to be elucidated (Fries 2010). The intracellular development of both *Nosema* species in the ventricular cells appears to be similar although *N. ceranae* seems to be less tissue specific than *N. apis* (De Graaf and Jacobs 1991; Chen *et al.* 2009a; Gisder *et al.* 2010). Using microscopic techniques, *Nosema* species spores were found in the ovaries and salivary, mandibular and hypopharyngeal glands (Steche 1960; Sokolov and Grobov 1963). Although the spores could not be identified to species level, because of the fairly recent emergence of *N. ceranae* in *A. mellifera*, it can be assumed that the spores were those of *N. apis*. Using conventional PCR and RFLP techniques, recent evidence showed that *N. ceranae* is not restricted to the midgut tissue but spread to other tissues including the hypopharyngeal glands and salivary glands, as well as the Malpighian tubules, brain and fat bodies (Chen *et al.* 2009a; Gisder *et al.* 2010). Although disease

biology and physiological responses to *Nosema* species have been well documented in other insect species, few studies have looked at the presence of *N. ceranae* and *N. apis* in honeybee glands and whether the parasites can complete their life cycle outside the ventricular cells.

Hypopharyngeal, salivary and mandibular glands play an important role in food processing and feeding the queens and larvae, suggesting that these glands could be another vehicle for horizontal food-borne transmission of *Nosema* species (Shen *et al.* 2005; Chen *et al.* 2006a, 2009a; Singh *et al.* 2010). In Hymenoptera, the venom sacs and ovipositors are used during defence. The common structural duct shared by the ovaries, an organ often containing *Nosema* species spores in insects (Alger and Undeen 1970; Fine 1984; Armstrong *et al.* 1986; Han and Watanabe 1988; Sajap and Lewis 1988; Siegel *et al.* 1988; Streett *et al.* 1993), and venom sacs strongly suggest that *Nosema* species may be also present in venom sacs as well as their glands; however, so far no studies have confirmed this evidence.

Multiplex quantitative RT-PCR (qPCR) is a sensitive technique that is capable of quantifying and differentiating the morphologically similar *N. ceranae* and *N. apis* simultaneously in a single sample (Chen *et al.* 2009b; Bourgeois *et al.* 2010; Traver and Fell 2011). This technique enables multiple target sequences to be analysed simultaneously in one sample, resulting in data that can be reliably compared. Although previous studies have identified *Nosema* species in different honeybee glands including the hypopharyngeal glands and thoracic salivary glands (Gilliam and Shimanuki 1967; Chen *et al.* 2009a; Gisder *et al.* 2010), no studies so far have quantified the spore load found within the glands of naturally infected forager bees or monitored their temporal patterns over an extended time period.

Infection of *Nosema* species by the ingestion of contaminated foods can be traced by examination of the Nosemosis status of the digestive tract, the gut (Fries 1988; Higes *et al.* 2007; Chen *et al.* 2009a). Therefore, the major motivation for this study was to monitor the nucleic acid levels in various honeybee glands of forager honeybees and attempt to correlate these levels to those found within the intestines of honeybees of the same hives. To do so, we developed a duplex real-time PCR assay using primers and TaqMan probes specific to either *N. ceranae* or *N. apis* to determine which *Nosema* species is present in the different gland tissues namely, the thoracic salivary, hypopharyngeal, mandibular glands, and the venom sac and glands and at what levels. Also, we describe for the first time the quantification of *N. ceranae* and *N. apis* in different gland tissues and show that the parasites follow seasonal patterns and are well correlated with those found in the intestines of the bees.

Materials and methods

Sample collection

Four hives located at an apiary at the Centre de Recherche en Sciences Animales de Deschambault (CRSAD) located in Deschambault (46·6734°N, 71·9169°W), Quebec, Canada were started in 2008 using free-mated sister *A. mellifera* hybrid Italian queens obtained from a local queen breeder (Les reines Moreau®, Saint-Liboire, QC, Canada) and 1·5 kg of worker bees. For the purpose of this study, we focused our efforts on studying the presence of *Nosema* species in forager bees; therefore, newly emerged bees that are usually *Nosema*-free were not sampled. Approximately 100 forager bees were collected from the side frames of the top super from each hive monthly basis during eight of the active months from July 2009 to July 2010 resulting in 32 collections. Hives were overwintered in a common environmentally controlled room (3–5°C and 30–40% RH) between from November 2009 to April 2010, during which no collections of bees were made. On 14th April 2010, hives were placed outdoors. Bees were euthanized by freezing them in liquid nitrogen and stored at −20°C until further use.

Tissue dissection

For each collection, the abdomens of 30 bees were dissected, pooled and ground in sterile water using a sterile mortar and pestle. The samples were then filtered using a 40-μm BD Falcon™ Cell Strainer (Cat no. 352340, MA; BD Biosciences, Mississauga, ON, Canada) to remove debris, and the presence and number of *Nosema* species spores in all the bee samples was identified using phase-contrast microscopy (600×) using a Bright-Line® Reichert 1492 haemocytometer (Cat no. 1492; Hausser Scientific, Horsham, PA, USA). Filtered samples were then pelleted by centrifugation at 8250 ***g*** for 12 min, the supernatant was discarded, and the pellet was used for DNA extraction. Following intestinal dissections, 15 of the 30 bees were used for gland dissection. Individual bees were dissected under an Olympus SZH dissecting microscope (40×) (Olympus America Inc., Center Valley, PA). The tissues of the mandibular glands, hypopharyngeal glands, thoracic salivary glands, venom sacs with venom glands and intestinal tracts (Fig. 1) were carefully dissected and separated from each bee using fresh forceps for each organ to prevent contamination. To ensure that minimal or no contamination from the haemolymph occurs, the isolated organs were washed twice with 1× PBS and rinsed three times with sterile ddH_2O to remove any remaining salts and to wash off any potentially contaminating haemolymph and stored at −80°C for DNA extraction.

DNA extraction

Fifty milligrams of 5-mm silica beads (Cat. no. 11079105; BioSpec Products, Inc., Bartlesville, OK, USA) and 400 μl buffer AP1 (Cat. no. 69104; Qiagen, Mississauga, ON, Canada) were added to intestinal samples, which were then lysed using a Precellys 24 (Bertin Technologies, Montigny-le-Bretonneux, France) for three cycles of 10 s each at 3360 ***g*** with 5 s pauses between cycles. The dissected glands were ground in liquid nitrogen in 1·5-ml microcentrifuge tubes using Scienceware® pestles (Cat. no. 19923-0000; Scienceware®, NJ, USA). DNA was isolated from all samples using the DNeasy Mini Plant kit (Cat. no. 69104; Qiagen) following the manufacturer's protocols. DNA was quantified using a NanoDrop ND-1000 Spectrophotometer (Thermo Scientific, Wilmington, DE, USA), and the quality was confirmed by running 100 ng of DNA on a 1% agarose (Cat. no. GO60-2; Applied Biological Materials Inc., Richmond, BC, Canada) gel electrophoresis.

Primers and probes

Already published species-specific primers specific for the 16SSU rDNA region for *N. ceranae* (218MITOC; GenBank accession no. DQ673615.1) and *N. apis* (NosApis; GenBank accession no. DQ235446.1) were synthesized by Alpha DNA (Montreal, QC, Canada) resulting in amplified products of 219 and 321 bp, respectively, and were used in conventional PCR assays throughout the study (Table 1). For duplex qPCR, species-specific primer pairs specific for the 16SSU rDNA region for *Nosema* species were designed by Integrated DNA Technologies (San Diego, CA, USA) and were HPLC purified, based on the previously published nucleotide sequences of *N. ceranae* (Nceranae; GenBank accession no. DQ486027.1) *N. apis* (Napis; GenBank accession no. U97150.1) resulting in respective amplified products of 250 and 269 bp (Table 1). Normalization of real-time qPCR data is critical for a reliable DNA quantification. The most common way to perform normalization is to relate the DNA level of the sample of interest to the DNA of a reference gene whose detection level is considered stable, regardless of cell type and across various experimental conditions (Thellin *et al.* 1999). Therefore, primers for the *A. mellifera* β-actin normalizing gene (GenBank accession no. AB023025.1) were designed to amplify a 181-bp product. The fluorophores HEX, with absorbance and emission

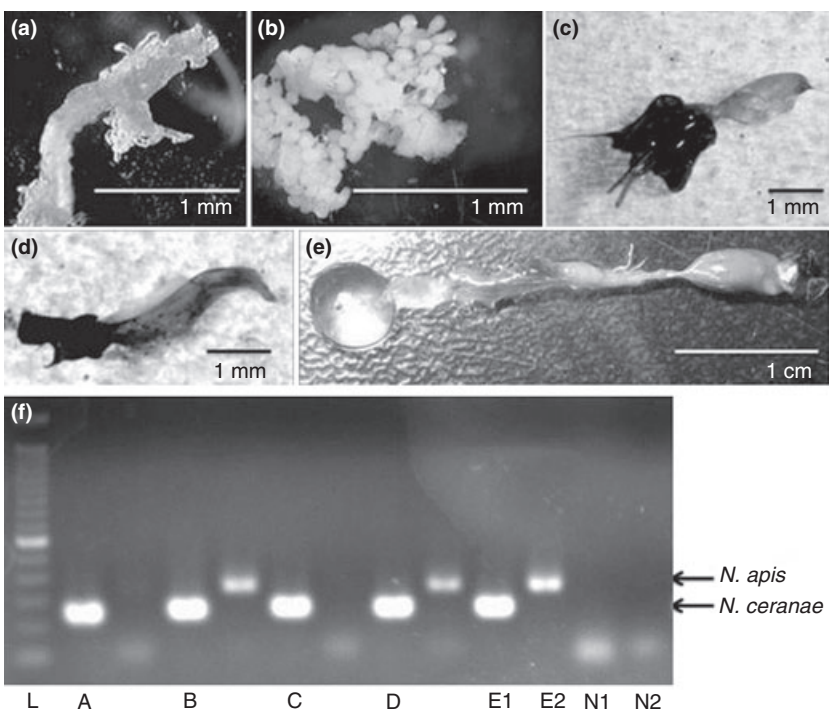

Figure 1 Dissections from *Apis mellifera* for *Nosema* species analysis: (a) salivary gland, (b) hypopharyngeal gland, (c) venom gland, (d) mandibular gland, (e) digestive tract. (f) Detection of *Nosema* spp. by polymerase chain reaction (PCR) amplification of nucleic acids from different tissues and examined for the presence of *Nosema ceranae* and *Nosema apis*. DNA was extracted from samples and subjected to PCR amplification using species-specific primers for *N. ceranae* (219 bp) and *N. apis* (321 bp). Positive samples were determined by 1·5% agarose gel electrophoresis. For each sample, *N. ceranae* then *N. apis* PCR products were loaded in neighbouring lanes. All samples were positive for *N. ceranae*, while the hypopharyngeal glands (b) and mandibular glands (d) showed co-detections. N1 indicates the negative control for *N. ceranae*, N2 for *N. apis*. E1 indicates the positive control for *N. ceranae*, and E2 for *N. apis*.

Table 1 Primers and probes specifications used for conventional and quantitative PCR amplification of *Nosema ceranae* and *Nosema apis*

Specificity	Primer	Sequence	Product size (bp)	Accession number	References
N. ceranae	218MitocF	5′-CGGCGACGATGTGATATGAAAATATTAA-3′	219	DQ673615.1	Martín-Hernández *et al.* (2007)
	218MitocR	5′-CCCGGTCATTCTCAAACAAAAAACCG-3′			
N. apis	321ApisF	5′-GGGGGCATGTCTTTGACGTACTATGTA-3′	321	DQ235446.1	Martín-Hernández *et al.* (2007)
	321ApisR	5′-GGGGGGCGTTTAAAATGTGAAACAACTATG-3′			
Apis mellifera	ActinF	5′-AGGAATGGAAGCTTGCGGTA-3′	181	AB023025.1	Chen *et al.* (2005)
	ActinR	5′-AATTTTCATGGTGGATGGTGC-3′			
	ActinProbe	5′-/56FAM/ATGCCAACACTGTCCTTTCTGGAGGTA/3IABkFQ/-3′			
N. ceranae	NceranaeF	5′-CGGATAAAAGAGTCCGTTACC-3′	250	DQ486027.1	Chen *et al.* (2009b)
	NceranaeR	5′-TGAGCAGGGTTCTAGGGAT-3′			
	NcerProbe	5′-/5HEX/CGTTACCCTTCGGGGAATCTTC/3IABkFQ/-3′			
N. apis	NapisF	5′-CCATTGCCGGATAAGAGAGT-3′	269	U97150.1	Chen *et al.* (2009b)
	NapisR	5′-CCACCAAAAACTCCCAAGAG-3′			
	NapisProbe	5′-/56FAM/ATAGTGAGGCTCTATCACTCCGCTG/3IABkFQ/-3′			

wavelengths of 535 and 556 nm, respectively, and FAM, with absorbance and emission wavelengths of 495 and 516 nm, respectively, were chosen for probe labelling because of their well-separated absorbance and emission wavelengths. Already published sequences were used for probe design and synthesized by Integrated DNA Technologies, (Table 1). The probe specific for *N. ceranae* was labelled with the HEX reporter dye at the 5′ end, while that for *N. apis* was labelled with the 6-FAM reporter dye at the 5′ end to allow for the amplification of both amplicons simultaneously in a duplex qPCR. Both probes were labelled with Iowa Black® FQ (Integrated DNA Technologies, Montreal, Canada) at the 3′ end, with absorbance and emission wavelengths of 531 and 620 nm, respectively, which has sufficient overlap to act as a quencher dye. The reference gene β-actin was labelled with the 6-FAM reporter dye at the 5′ end and Iowa Black® FQ quencher dye at the 3′ end and used in a separate reaction from the *Nosema* species. All primers (Table 1) were first tested in conventional PCR assays to confirm that the designed primers amplify only the target and reference genes and the amplified products were sequenced and compared with sequences deposited in the GenBank database of NCBI.

Conventional PCR

DNA extracted from all samples was tested with primers sets specific to *N. ceranae*, *N. apis* and *A. mellifera* actin in separate PCRs. Each reaction contained 1× PCR buffer, 2 mmol l^{-1} $MgCl_2$, 0·2 mmol l^{-1} each dNTP, 0·2 μmol l^{-1} each primer, 0·5 U recombinant Taq DNA polymerase (Fermentas, Burlington, ON, Canada) and either 250 ng DNA from bee intestines or 25 ng DNA from glands in a total volume of 12·5 μl. The thermal cycling conditions were as follows for all primer sets: one cycle of initial denaturation at 95°C for 10 min, followed by 35 cycles of denaturation at 95°C for 30 s, annealing at 60°C for 30 s and extension at 72°C for 30 s, followed by one cycle of final extension at 72°C for 7 min using a GeneAmp® PCR System 9700 (Applied Biosystems, Streetsville, ON, Canada). All primer sets were run with a positive control and a negative control containing no template DNA. All samples were run on a 1% agarose (Cat. no. GO60-2; Applied Biological Materials, Inc.) gel electrophoresis. The specificity of the PCR products was confirmed by purifying the PCR products by standard desalting using the QIAquick PCR Purification kit (Cat. no. 28140; Qiagen) and was sequenced at Genome Quebec (Montreal, QC, Canada). Sequences were compared with results deposited in the GenBank database of NCBI.

Recombinant plasmid DNA and standard curve construction

Purified *A. mellifera* actin amplicons were incorporated into a pCR2.1-TOPO® vector (Cat. no. KNM455001; Invitrogen, Carlsbad, CA, USA) following the manufacturer's protocols. Purified *N. apis* and *N. ceranae* amplicons were each incorporated into pUC57 vector and cloned using the TOPO® TA-cloning kit (Cat. no. KNM455001; Invitrogen) following the manufacturer's protocols. Plasmid DNA was purified using the PureLink™ Quick Plasmid Miniprep kit (Cat. no. K210010; Invitrogen) and sent for sequencing at Genome Quebec. Sequences were compared with results deposited in the GenBank database of NCBI. The copy number of plasmid was calculated based on the concentration of purified plasmid DNA and the molecular mass of the plasmid (vector plus amplicon). A standard curve for *A. mellifera* actin was constructed based on the following copy numbers: 10^9, 10^8, 10^7, 10^6, 10^5 and 10^4, which is the range of actin copy numbers in the bee intestines. Separate *Nosema* species standards were constructed

for the simplex qPCR assays containing the following copy numbers: 10^9, 10^8, 10^7, 10^6, 10^5, 10^4, 10^3, 10^2 and 10^1, which spanned the infection levels of all samples. The sensitivity of the assays was determined by plotting the log-initial quantity of each dilution against the corresponding threshold value (C_t). The amplification efficiency of each standard was calculated from the slope of each standard as follows: $E = 10^{(-1\text{slope}-1)} - 1$. Once optimized, the standards were combined for duplex qPCRs using the same copy numbers per reaction as for simplex. The reaction was then optimized until the efficiencies and C_t values were similar to those for simplex. It was ensured that sensitivity was maintained by performing a duplex reaction with 10^9 copies of *N. apis* in combination with 10^2 copies of *N. ceranae* and vice versa to make certain that high amounts of one species did not inhibit the amplification of lower titres of the other species.

Duplex quantitative real-time PCR

The nucleic acid levels of *N. ceranae* and *N. apis* were quantified in all samples (i.e. intestines and glands) by duplex qRT-PCR using the Stratagene MxPro 3005 (Agilent Technologies, Cedar Creek, TX). Each *Nosema* duplex amplification mixture contained 1× PCR buffer, 2·5 mmol l^{-1} $MgCl_2$, 0·4 mmol l^{-1} each dNTP, 0·3 μmol l^{-1} each primer, 0·15 μmol l^{-1} each probe, 2 μmol l^{-1} ROX, 1·5 U recombinant Taq DNA polymerase (Fermentas) and either 250 ng DNA from bee intestines or 25 ng DNA from glands in a total volume of 25 μl. *Apis mellifera* actin was amplified in a separate mixture containing 1× PCR buffer, 2·5 mmol l^{-1} $MgCl_2$, 0·4 mmol l^{-1} each dNTP, 0·2 μmol l^{-1} each primer, 0·075 μmol l^{-1} probe, 2 μmol l^{-1} ROX, 1·0 U recombinant Taq DNA polymerase (Fermentas) and either 250 ng DNA from bee intestines or 25 ng DNA from glands in a total volume of 25 μl. Actin and *Nosema* species qPCRs were run on the same plate for all samples. All qPCRs were run under the following conditions: one cycle of initial denaturation at 94°C for 10 min, followed by 45 cycles of denaturation at 95°C for 30 s, annealing at 55°C for 30 s and extension at 68°C for 30 s. Standard curves and no template controls were run with each plate. All samples were performed in triplicate technical runs. Amplification results were expressed as the threshold cycle (C_t) value and converted to copy numbers by plotting the C_t values against the standard curve. The coefficient of variation was calculated for each sample to ensure repeatability of amplification. Samples with a coefficient of variation above 1·0 had their outliers removed. The specificity of the duplex qPCR was confirmed by gel electrophoresis and sequence analysis to verify the correct size and specificity of the qPCR products.

Statistical analysis

The coefficient of correlation (r) values was calculated, using the pairwise method, to compare the spore loads within the glands to those in the bee intestines to determine whether a relationship between the gland spore loads and intestinal infection levels exists (JMP 8; SAS Institute, Inc., NC, USA). Outliers were determined using the Jacknife distance method and removed (JMP 8). Additionally, principle component analysis (PCA) was performed with all glands and bee samples using SIMCA-P$^+$ 12.0 software (Umetrics; MKS Instruments Inc., Andover, MA) to validate the correlation analyses.

Results

DNA extraction from honeybee intestines and gland tissues demonstrated high quality and yield of DNA (data not shown) that could successfully be amplified by conventional PCR using the 16S rRNA species-specific primers for *N. ceranae*, *N. apis* and β-actin primers for *A. mellifera* with the expected respective amplicon sizes of 219, 321 and 181 bp (Fig. 1). β-Actin was amplifiable in all samples, demonstrating that samples tested negative for either *Nosema* species were not causing PCR inhibition and represent true negatives (data not shown).

The duplex qPCR assay was optimized until the efficiencies and sensitivities of both *Nosema* targets were approximately equal. Optimization was done originally on simplex reactions such that the efficiencies were 102·3 and 98·0% for *N. ceranae* and *N. apis*, respectively, while those for the duplex reactions were 101·9 and 96·6%, respectively, demonstrating reproducibility between the simplex and duplex reactions. The sensitivity of each reaction was also similar in simplex *vs* duplex reactions at 100 copies per reaction and 70 copies per reaction for *N. ceranae* and *N. apis*, respectively, demonstrating a lower threshold than the traditional microscope-based spore count method with a threshold of 10 000 spores per bee. The R^2 value demonstrates the linearity of the standard curves and was calculated to be 0·995 and 0·993 for *N. ceranae* and *N. apis*, respectively, in the duplex reaction. The coefficient of variation was low for both *N. ceranae* (0·91, $n = 129$) and *N. apis* (1·05, $n = 129$) demonstrating reproducibility of the duplex qPCR (data not shown).

β-Actin was performed in a simplex reaction and had an efficiency of 99·1% and a R^2 of 0·989. Equal amounts of actin (*c.* 508 550 copies per bee) were detected in the bee intestine samples, while equal amounts were found in the hypopharyngeal glands (*c.* 67 500 copies per set of glands), mandibular glands (*c.* 40 800 copies per set of glands), salivary glands (*c.* 43 200 copies per set of

glands) and venom sac and glands (*c.* 60 900 copies per set), demonstrating that similar titres of DNA were found in each tissue type (data not shown).

Almost 60% of the collections produced mixed infections in honeybee intestines. Both microsporidian fungi were present as single and mixed species in all gland tissues with the exception of the salivary glands, which contained *N. ceranae* only or both species, but never *N. apis* alone (Table 2). In all cases of mixed-species detection, *N. ceranae* gene copies substantially (8·0-fold increase) out numbered those of *N. apis*. More than 70% of the mandibular and salivary glands produced mixed-species detections, followed by 55% in the hypopharyngeal and venom glands (Table 2). The per cent distribution of *N. ceranae* as single-species detection in different glands was highest in venom glands and hypopharyngeal glands (41% of total positive samples) followed by the salivary glands (29%) and mandibular glands (26%).

Significant correlations ($P < 0{\cdot}05$) between all gland and honeybee intestine nucleic acid levels for both microsporidian species, except for *N. ceranae* in the hypopharyngeal glands, were observed (Fig. 2). A strong correlation was established between all glands and bee intestines for *N. apis* and between the venom sacs and glands, salivary and mandibular glands and bee intestines for *N. ceranae* (Fig. 2). PCA confirmed the correlation values for *N. ceranae* as the stingers and intestinal samples were closely located on the plot, while those for the remaining tissues contained *N. ceranae* spores and were located in a different quadrant (Fig. 3). The separation of the different tissues appears to be based on their location in the honeybee body with the tissues located at the anterior end of the body clustering tightly together and those at the posterior end grouping together. PCA for *N. apis* demonstrated a close relationship among all of the glands, while the intestinal tissues were located in a different region of the graph, suggesting that causes of variation are slightly different for these tissues and that the infections may in fact be more tissue specific.

Overall, the average number of copies that correspond to the parasite spore load for both *N. ceranae* and *N. apis* were highest in spring and early summer and lower in late summer and fall for intestinal and gland tissues, with *N. apis* also peaking in late fall (Fig. 4). However, spore loads in the intestines were always higher than those in the glands for both *N. ceranae* and *N. apis* (Fig. 4). Seasonal patterns of *N. ceranae* and *N. apis* nucleic acid levels were similar in all of the glands and followed similar patterns to those in the intestines. Typically, when levels increased or decreased in the intestines, the levels increased or decreased within the glands (Fig. 4). These results are consistent throughout the 8 months of collection and suggest that sampling time did not affect the correlation values (Fig. 4). *Nosema ceranae* was detected during every month in most hives in most tissue types, while *N. apis* was less prevalent (Fig. 4).

Discussion

Honeybee glands, which are important in producing honey and bee bread, as well as for feeding and communication, may be important in disease epidemiology and horizontal transmission of diseases (Shen *et al.* 2005; Chen *et al.* 2006a,b). Studies have identified *N. ceranae* and *Nosema* sp. spores, presumably belonging to *N. apis*, in different glands (Steche 1960; Sokolov and Grobov 1963; Chen *et al.* 2009a; Gisder *et al.* 2010), but did not quantitatively monitor the presence of both species in these glands. Our study represents the first report on the molecular detection and quantification of both *Nosema* species in hypopharyngeal glands, mandibular glands, thoracic salivary glands and venom sacs in the European honeybee using multiplex qPCR. The developed method in this study has proven to be specific, reliable and sensitive with threshold levels of 100 copies per reaction for *N. ceranae* and 70 copies per reaction for *N. apis*. These limits are comparable to those found in multiplex qPCR assays for *Nosema* species (Chen *et al.* 2009b; Bourgeois

Table 2 Positive *Nosema* spp. samples in honeybee glands and intestines using duplex qPCR and expressed as per cent of total positive samples

	Nosema ceranae	*Nosema apis*	Co-detections	Total positive samples
Hypopharyngeal glands	11 (40·7%)	1 (3·7%)	15 (55·6%)	27 (84·4%)
Mandibular glands	6 (26·1%)	1 (4·3%)	17 (73·9%)	23 (71·9%)
Salivary glands	7 (29·2%)	0 (0·0%)	17 (70·8%)	24 (75·0%)
Venom sacs and glands	12 (41·4%)	1 (3·4%)	16 (55·2%)	29 (90·6%)
Intestinal tract	11 (34·4%)	2 (6·2%)	19 (59·4%)	32 (100%)

Numbers represent single *Nosema* spp. infections (*N. ceranae* or *N. apis* only) or mixed infections (*N. ceranae* and *N. apis*). A total of 32 collections were carried out for each sample type. Intestines were dissected from 30 bees per sample, while each gland type was dissected from 15 of the 30 bees. Numbers in brackets for single and co-detections represent the percentage of samples that were positive for *Nosema* nucleic acids in comparison with the total number of positive samples. Numbers in brackets for total positive samples are the percentages of positive samples in comparison with the number of total samples.

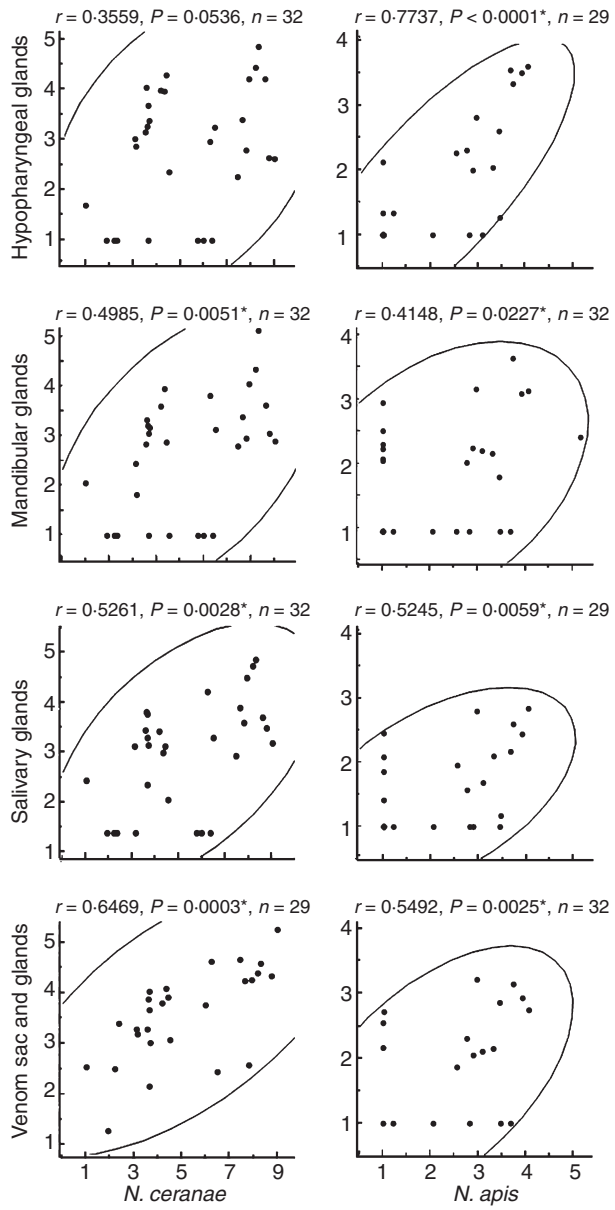

Figure 2 Correlation analyses of intestinal tract copy numbers (per bee) *vs* the different gland tissue copy numbers (per set of glands). Copy numbers were calculated by converting the duplex qPCR C_t values to copy numbers using the standard curve method. Correlation analyses were carried out using the pairwise method and outliers removed using Jacknife distances (jmp 8). Data were log(x + 1) transformed. Correlations are plotted with gland values (per set of glands) on the y-axis *vs* intestine values (per bee) on the x-axis. *Significant correlation values (P < 0·05).

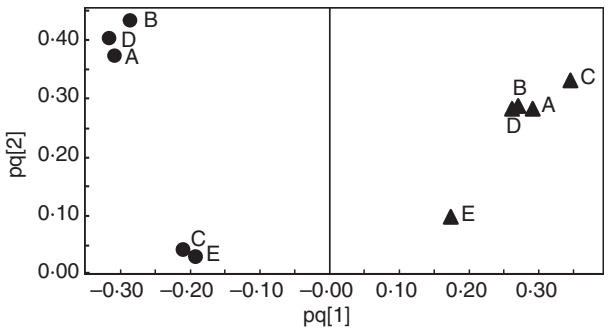

Figure 3 Principle component analysis (PCA) of *Nosema ceranae* and *Nosema apis* copy numbers in different gland and intestinal tissues. Groupings were made for each *Nosema* species by grouping all samples (n = 32) for each gland or intestines together to strengthen the analysis and eliminate the factor of sampling time. PCA was carried out using SIMCA-P$^+$ 12.0 software (Umetrics). (A) Salivary glands, (B) hypopharyngeal glands, (C) venom sacs and glands, (D) mandibular glands, (E) intestines where closed circles indicate *N. ceranae* and closed triangles indicate *N. apis*.

et al. 2010; Traver and Fell 2011). Additionally, the duplex method provided simultaneous detection and quantification of both *Nosema* species within the different glands that cannot be accomplished by other current molecular methods. One may argue that the detection of *Nosema* species nucleic acids within the glands may be the result of contamination by the haemolymph. To eliminate this uncertainty and minimize the risk of contamination, extra care was taken that clean sterile dissection tools were used for each sample and all tissue types were rinsed twice in sterile 1× PBS buffer followed by three rinses in sterile water. This routine practice ensured that the nucleic acids originate from within the glands tested. Additionally, the fact that some gland samples tested negative for the presence of either *Nosema* spp. during certain months is an indication that the dissection method we have adopted was effective in eliminating sources of contamination.

Significant correlative relationships between the nucleic acid levels of *N. ceranae* and *N. apis* between the glands and the intestines demonstrate the extent of both diseases within the colonies. Although microscope studies of the tissues were not attempted in this study, the results clearly demonstrate that spore loads within the glands are altered by the hive infection levels and that disease transmission via these glands may be possible and may differ depending on colony infection levels. All the food, including royal jelly, honey and bee bread, as well as wax are partly composed of glandular secretions of the hypopharyngeal glands, thoracic salivary glands and mandibular glands (Shen *et al.* 2005; Chen *et al.* 2006a). The presence of both *N. ceranae* and *N. apis* in these glands greatly suggests that food production and the building of comb can act as sinks and sources for both *Nosema* species and may increase the likelihood of disease dispersal via horizontal transmission within the hive as well as to the

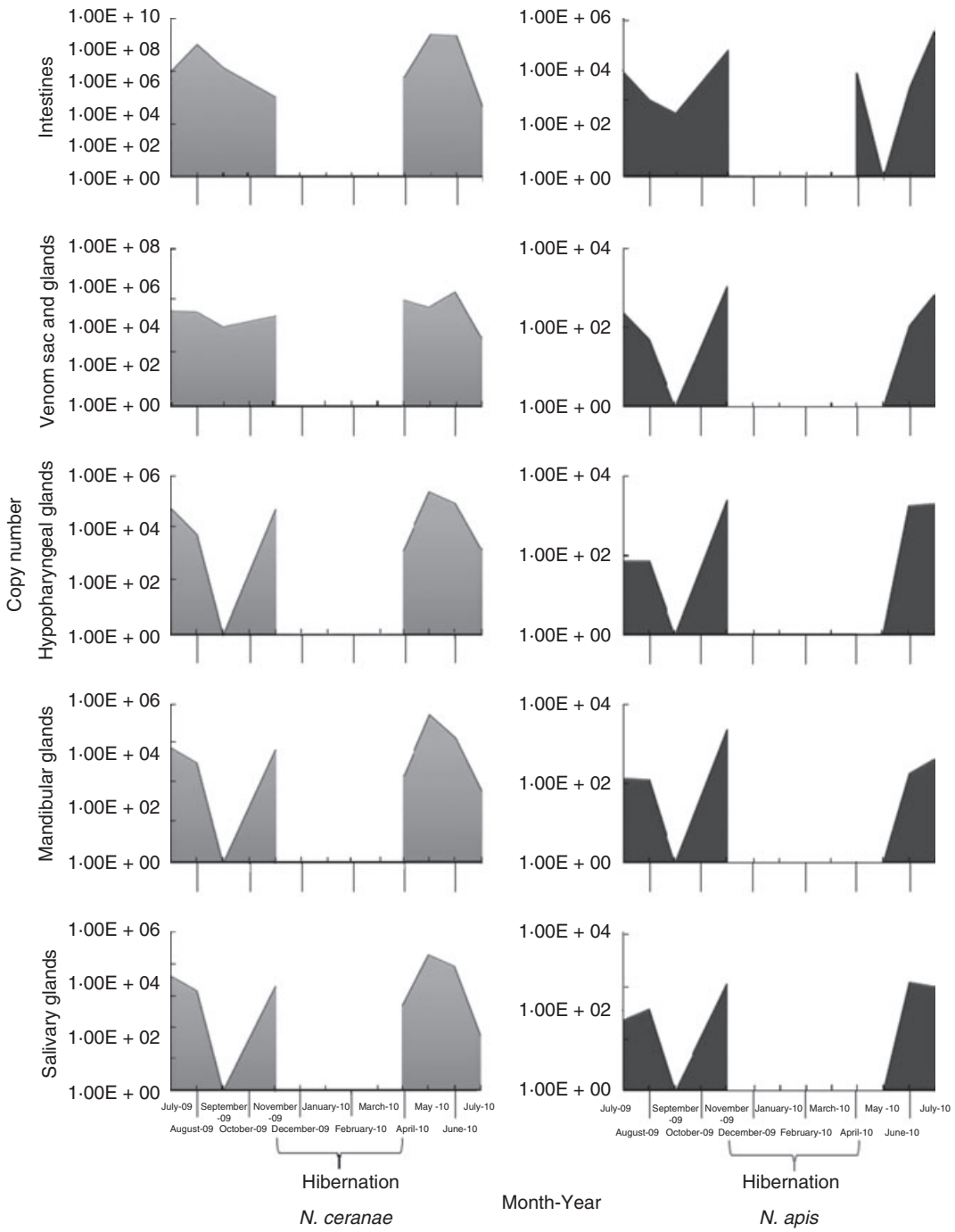

Figure 4 Average monthly distribution of *Nosema ceranae* (■) and *Nosema apis* (■) in bee intestines and different gland tissues from July 2009 to July 2010. Copy numbers are represented as the average copy number per bee for bee intestines or per set of glands and were calculated by converting the duplex qPCR C_t values to copy numbers using the standard curve method. Months with copy numbers at 1·0E + 0 indicate average copy numbers of zero for the given month with β-actin being detected for all samples.

queen. Support for glandular secretions, being a route of transmission of honeybee viruses, has been demonstrated by several studies (Bailey 1968; Shen *et al.* 2005; Chen *et al.* 2006a; Giersch *et al.* 2009; Singh *et al.* 2010). Of interest is the presence of both species in the venom glands, which has not been demonstrated previously, and the significance of this discovery merits further investigation. The possible role for venom sacs in the transmission

of *Nosema* spp. remains unclear and merits further investigation. PCA demonstrated that the factors leading to differences between *N. ceranae* and *N. apis* nucleic acid levels in the different glands appear to be influenced by the location of the glands within the honeybee's body (anterior *vs* posterior tissues) in the case of *N. ceranae*, while those of *N. apis* suggest tissue specificity as the intestines grouped separately from the glands. Although the exact reasons for these separations warrant further investigation, these data support previous studies that describe *N. ceranae* as less tissue specific than *N. apis* (De Graaf and Jacobs 1991; Chen *et al.* 2009a; Gisder *et al.* 2010).

The incidence and seasonality of *Nosema* species infections have been described in honeybees although seasonal patterns have been disputed for *N. ceranae* and remain to be conclusively verified (Bailey 1955; Martín-Hernández *et al.* 2007; Fries 2010; Gisder *et al.* 2010; Runckel *et al.* 2011; Traver and Fell 2011). Seasonal patterns for *N. ceranae* infection levels were higher in the spring and lower in the fall in the intestines, while the gland levels were high in the spring with a second peak in the fall. These results are consistent with recently published findings (Gisder *et al.* 2010; Runckel *et al.* 2011; Traver and Fell 2011). Different seasonal patterns for *N. apis* were observed and are similar to those previously reported (Bailey 1955; Fries 2010), which show low prevalence levels during the summer with a small peak in the fall followed by an increase in the spring. The reason(s) for the similar patterns and correlation values between the intestinal infection levels and the gland spore loads remains unclear and merits further study.

In this study, the quantification of specific nucleic acids of both *Nosema* species in the glands by duplex qPCR confirms that spores and/or the vegetative stage of *Nosema* species are present within the glands and highly suggests that these tissues may be infected; however, evidence that spores become trapped or replicate in these tissues is still lacking. On the other hand, many microsporidian species infect multiple tissues of other bees. The microsporidian *Nosema bombi*, a parasite of different bumblebee species, completes its life cycle in the ventricular cells as well as the Malpighian tubules, fat body cells, the brain and nerve tissue cells (Fries *et al.* 2001). Thus, it is probable that *N. ceranae* and *N. apis* may be able to complete their life cycle outside the ventricular cells, but this notion requires further research.

In summary, this is the first study to differentiate and reliably quantify the temporal levels of *Nosema* species in different gland tissues of honeybees using duplex qPCR. Furthermore, our study has demonstrated that both *Nosema* species are not only present in tissues, but that their prevalence in these tissues is correlated with the overall infection levels of the intestines. Both species can be detected simultaneously in an individual honeybee and could be amplified in different gland tissues, potentially making these tissues a new infection reservoir for *N. ceranae* and *N. apis*. More than 50% of the infected bee samples had both species, suggesting that these species could infect the same honeybee simultaneously with higher levels of *N. ceranae* in all gland tissues. These results are consistent with previously published data that demonstrate a higher prevalence of *N. ceranae* (Klee *et al.* 2007; Martín-Hernández *et al.* 2007; Traver and Fell 2011).

Acknowledgements

We would like to thank Pierre Giovenazzo, Emile Houle and members of the CRSAD team at Dechambault, Quebec, for providing the samples for this project and Dr Terry Wheeler for his technical assistance. We also thank Dr K. Alifevis for conducting the PCA analysis. This work was supported by the Ministère d'agriculture, pêcheries *et* alimentation de Québec (MAPAQ) and in part by the Natural Sciences and Engineering Research Council (NSERC).

References

Alger, N.E. and Undeen, A.H. (1970) The control of a microsporidian, *Nosema* sp., in an anopheline colony by an egg-rinsing technique. *J Invertebr Pathol* **15**, 231–327.

Armstrong, E., Bass, L., Staker, K. and Harrell, L. (1986) A comparison of the biology of a *Nosema* in *Drosophila melanogaster* to *Nosema kingi* in *Drosophila willistoni*. *J Invertebr Pathol* **48**, 124–126.

Bailey, L. (1955) The epidemiology and control of *Nosema* disease of the honey bee. *Ann Appl Biol* **43**, 379–389.

Bailey, L. (1968) Honey bee pathology. *Annu Rev Entomol* **13**, 191–212.

Bourgeois, A., Rinderer, T., Beaman, L. and Danka, R. (2010) Genetic detection and quantification of *Nosema apis* and *N. ceranae* in the honey bee. *J Invertebr Pathol* **103**, 53–58.

Chen, Y.P., Higgins, J.A. and Feldlaufer, M.F. (2005) Quantitative real-time reverse transcription PCR analysis of deformed Wing virus infection in the honeybee (*Apis mellifera* L.). *Appl Environ Microbiol* **71**, 436–441.

Chen, Y., Evans, J. and Feldlaufer, M. (2006a) Horizontal and vertical transmission of viruses in the honey bee, *Apis mellifera*. *J Invertebr Pathol* **92**, 152–159.

Chen, Y., Pettis, J., Collins, A. and Feldlaufer, M. (2006b) Prevalence and transmission of honeybee viruses. *Appl Environ Microbiol* **72**, 606–611.

Chen, Y., Evans, J., Murphy, C., Gutell, R., Zuker, M., Gundensen Rindal, D. and Pettis, J. (2009a) Morphological, molecular, and phylogenetic characterization of *Nosema ceranae*, a microsporidian parasite isolated from the

european honey bee, *Apis mellifera*. *J Eukaryot Microbiol* **56**, 142–147.

Chen, Y., Evans, J., Zhou, L., Boncristiani, H., Kimura, K., Xiao, T., Litkowski, A. and Pettis, J. (2009b) Asymmetrical coexistence of *Nosema ceranae* and *Nosema apis* in honey bees. *J Invertebr Pathol* **101**, 204–209.

De Graaf, D. and Jacobs, F. (1991) Tissue specificity of *Nosema apis*. *J Invertebr Pathol* **58**, 277–278.

Fine, P.E.M. (1984) Vertical transmission of pathogens in invertebrates. In *Comparative Pathology, Vol. 7, Pathogens of Invertebrates: Application in Biological Control and Transmission Mechanisms* ed. Cheng, T.C. pp. 205–241. New York: Plenum Press.

Fries, I. (1988) Infectivity and multiplication of *Nosema apis* Z. in the ventriculus of the honey bee. *Apidologie* **19**, 319–328.

Fries, I. (2010) *Nosema ceranae* in European honey bees (*Apis mellifera*). *J Invertebr Pathol* **103**, S73–S79.

Fries, I., De Ruijter, A., Paxton, R.J., DaSilva, A.S., Slemenda, S.B. and Pieniazek, N.J. (2001) Molecular characterization of *Nosema bombi* (Microsporidia: Nosematidae) and a note on its sites of infection in *Bombus terrestris* (Hymenoptera: Apoidea). *J Apic Res* **40**, 91–96.

Giersch, T., Berg, T., Galea, F. and Hornitzky, M. (2009) *Nosema ceranae* infects honey bees (*Apis mellifera*) and contaminates honey in Australia. *Apidologie* **40**, 117–123.

Gilliam, M. and Shimanuki, H. (1967) In vitro phagocytosis of *Nosema apis* spores by honey-bee hemocytes. *J Invertebr Pathol* **9**, 387–389.

Gisder, S., Hedtke, K., Mockel, N., Frielitz, M., Linde, A. and Genersch, E. (2010) Five-year cohort study of *Nosema* spp. in Germany: does climate shape virulence and assertiveness of *Nosema ceranae*? *Appl Environ Microbiol* **76**, 3032–3038.

Han, M. and Watanabe, H. (1988) Transovarial transmission of two microsporidia in the silkworm, *Bombyx mori*, and disease occurrence in the progeny population. *J Invertebr Pathol* **51**, 41–45.

Higes, M., García-Palencia, P., Martín-Hernández, R. and Meana, A. (2007) Experimental infection of *Apis mellifera* honeybees with *Nosema ceranae* (Microsporidia). *J Invertebr Pathol* **94**, 211–217.

Higes, M., Martín Hernández, R., Botías, C., Bailón, E., González Porto, A., Barrios, L., Del Nozal, M., Bernal, J. *et al.* (2008) How natural infection by *Nosema ceranae* causes honeybee colony collapse. *Environ Microbiol* **10**, 2659–2669.

Keeling, P. and Fast, N. (2002) Microsporidia: biology and evolution of highly reduced intracellular parasites. *Annu Rev Microbiol* **56**, 93–116.

Klee, J., Besana, A., Genersch, E., Gisder, S., Nanetti, A., Tam, D., Chinh, T., Puerta, F. *et al.* (2007) Widespread dispersal of the microsporidian *Nosema ceranae*, an emergent pathogen of the western honey bee, *Apis mellifera*. *J Invertebr Pathol* **96**, 1–10.

Martín-Hernández, R., Meana, A., Prieto, L., Salvador, A., Garrido-Bailon, E. and Higes, M. (2007) Outcome of colonization of *Apis mellifera* by *Nosema ceranae*. *Appl Environ Microbiol* **73**, 6331–6338.

Mayack, C. and Naug, D. (2009) Energetic stress in the honeybee *Apis mellifera* from *Nosema ceranae* infection. *J Invertebr Pathol* **100**, 185–188.

Mayack, C. and Naug, D. (2010) Parasitic infection leads to decline in hemolymph sugar levels in honeybee foragers. *J Insect Physiol* **56**, 1572–1575.

Runckel, C., Flenniken, M.L., Engel, J.C., Ruby, J.G., Ganem, D., Andino, R. and DeRisi, J.L. (2011) Temporal analysis of the honey bee microbiome reveals four novel viruses and seasonal prevalence of known viruses, *Nosema*, and *Crithidia*. *PLoS ONE* **6**, e20656–e20673.

Sajap, A.S. and Lewis, L.C. (1988) Histopathology of transovarial transmission of *Nosema pyrausta* in the European corn borer, *Ostrinia nubilalis*. *J Invertebr Pathol* **52**, 147–153.

Shen, M., Cui, L., Ostiguy, N. and Cox-Foster, D. (2005) Intricate transmission routes and interactions between picorna-like viruses (Kashmir bee virus and sacbrood virus) with the honeybee host and the parasitic varroa mite. *J Gen Virol* **86**, 2281–2289.

Siegel, J.P., Maddox, J.V. and Ruesink, W.G. (1988) Seasonal progress of *Nosema pyrausta* in the European corn borer, *Ostrinia nubilalis*. *J Invertebr Pathol* **52**, 130–136.

Singh, R., Levitt, A.L., Rajotte, E.G., Holmes, E.C., Ostiguy, N., Lipkin, W.I., Toth, A.L. and Cox-Foster, D.L. (2010) RNA viruses in hymenopteran pollinators: evidence of inter-taxa virus transmission via pollen and potential impact on non-*Apis* Hymenopteran species. *PLoS ONE* **5**, e14357. doi: 10.1371/journal.pone.0014357.

Sokolov, V.P. and Grobov, O.F. (1963) *Nosema* spores in the hemolymph of the bee. *Pchelovodstvo* **7**, 39.

Steche, W. (1960) Åtiologie und therapie der nosematose der honigbiene. *Zeitung Bienenfarsche* **5**, 49–52.

Streett, D.A., Woods, S.A. and Onsager, J.A. (1993) Vertical transmission of a *Nosema* sp. (Microsporidia: Nosematidae) infecting a grasshopper, *Chorthippus curtipennis* (Orthoptera: Acrididae). *Environ Entomol* **22**, 1031–1034.

Thellin, O., Zorzi, W., Lakaye, B., De Borman, B., Coumans, B., Hennen, G., Grisar, T., Igout, A. and Heinen, E. (1999) Housekeeping genes as internal standards: use and limits. *J Biotech* **75**, 291–295.

Traver, B.E. and Fell, R.D. (2011) Prevalence and infection intensity of *Nosema* in honey bee (*Apis mellifera* L.) colonies in Virginia. *J Invertebr Pathol* **107**, 43–49.